BODY DESIGN OF TENDON-DRIVEN JUMPING ROBOT USING SINGLE ACTUATOR AND WIRE SET

T. TAKUMA*, K. TAKAI*, Y. IWAKIRI* and W. KASE*

** Osaka Institute of Technology,*
Osaka 5358585, Japan
E-mail: takashi.takuma@oit.ac.jp

Although a mechanism in which a single actuator and a wire passing through pulleys drive the joints is a strong candidate for realizing the dynamic behavior because of its appropriate weight and simple mechanism, the problem arises that the position of the pulley influences the dynamic behavior. This paper is focused on vertical jumping. In our research, we searched an appropriate set of positions of a pulley considering the practical development of the robot and derived the relationship between the position of the pulley and the force on the tips of the robot's foot for jumping. Simulation results suggest the possibility that some sets of positions allow an error in the attachment of the pulley, and the derived relationship indicates that the ratio of the pulling force of wire and vertical force on the ground strongly constrain the position of the pulley.

Keywords: Tendon-driven robot, vertical jumping, body design

1. Introduction

One of the challenging issues presented by the design of legged robots is the realization of dynamic motion, such as jumping and running. In order to lift a heavy robot body, in conventional approaches, an electric servo motor drives each joint. However, a motor that generates relatively high force is heavy and further increases the robot's weight, which causes its joints or motor to break. One of the key mechanisms for achieving such a motion is a body design in which the robot is equipped with a minimal number of an actuator. For realizing a robot driven by minimal number of actautor, Günter and Iida proposed a unique monopod hopper equipped with a large curved foot driven by only one motor.[1] In many studies, an interlock mechanism using light weight elastic materials was adopted[2,3] A tendon-driven system in which a wire to drive the joint(s) is pulled by an actuator is a suitable mechanism for achieving a light weight robot. In such a tendon-driven mechanism, the wire passes through pulleys attached on the links, and torques to rotate the joints are generated, depending on three

H. Montes et al. (eds.), *CLAWAR 2018: 21st International Conference on Climbing and Walking Robots and the Support Technologies for Mobile Machines,*
Robotics Transforming the Future

factors: the amount of pulling force, the length of the moment arm between the joint and the pulley, and the angle between the moment arm and the direction of the pulling force. Therefore, it is very important to examine the position of the pulley, which determines the angle between the moment arm and the pulling force.

By utilizing a tendon-driven mechanism, we aim to achieve successful vertical jumping. In this study, we investigated two issues related to the design of the tendon-driven robot, in particular to the position of the pulley: searching the position of the pulley for realizing the vertical jumping, and the formulation of a relationship between the position of the pulley and the force added on the toe for determining candidates of the pulley position. To examine the former issue, a simulation was conducted. In the simulation, an appropriate set of the possible positions of the pulley was searched, and the area in which the appropriate pulley positions were gathered was then extracted considering the practical development of the robot. To address the latter issue, we determined the condition of the position of the pulley required to realize vertical jumping by utilizing a mathematical model of the position of the pulley and the reaction force at the working point.

2. Model configuration

2.1. *Frame model*

Figure 1(a) shows the frame of the robot and the driving mechanism consisting of a single actuator and a wire set. The model has four links: the trunk, thigh, shank, and foot. It has three joints: the hip, knee, and ankle. The lengths of the links are denoted by l_1 – l_4, respectively, and torques of the hip, knee, and ankle are denoted by τ_1, τ_2, and τ_3, respectively. The angle is denoted by θ_i. For further simulation and derivation of the relationship between the positions of the pulley and a reaction force, we set the coordinate system Σ_0: the origin is set on the tips of the trunk, the Y_0 axis is set along the trunk link, and the X_0 axis is perpendicular to the Y_0 axis, as shown in Figure 1(b). The positions of the pulley and end point of the wire are labeled P_i^a (i = 0, 1, 2, 3) and the joints are labeled P_j (j = 1, 2, 3). Note that the point where the wire is attached to the actuator is P_0^a and the other endpoint of the wire is P_3^a. P_1^a is attached to the thigh and P_2^a is attached to the shank link. In this paper, the position of the attaching point P_0^a did not move when the actuator pulled the wire, although the actual linear actuator does move while pulling the wire. P_1, P_2, and P_3 correspond to the hip, knee, and ankle joint, respectively. The coordinate of

P_i^a is defined based on Σ_0 when the model stands vertical to the ground as $(x_t, y_t)^T$, $(x_h, y_h)^T$, $(x_k, y_k)^T$, and $(x_a, y_a)^T$ [mm], respectively. The coordinate of P_j is also defined based on Σ_0 as $(x_1, y_1)^T$, $(x_2, y_2)^T$, and $(x_3, y_3)^T$ [mm], respectively. As shown in the figure, the pulley or endpoint is set at the front side when $x_*(* = t, h, k, a) > 0$. y_* is negative when the pulley or endpoint is set below the origin of Σ_0. $\mathbf{e}_k$ $(k = 1, 2, 3)$ is a unit vector of tensional force on the pulley P_i^a and T is the magnitude of pulling force of the actuator.

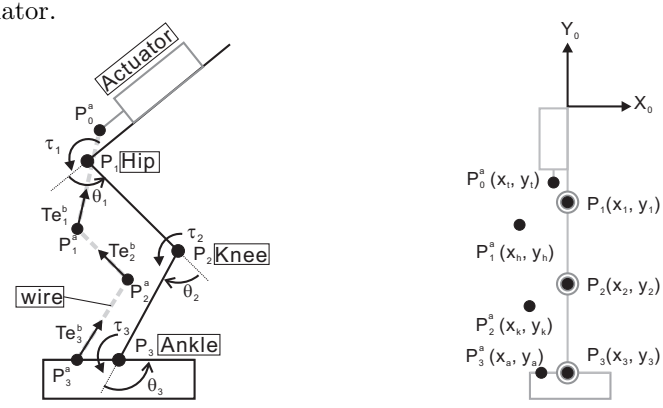

(a) Joint configuration, position of pulley, joint angle, and torque

(b) Definition of coordinate system

Fig. 1. Tendon-driven jumping robot using single set of actuator and wire

2.2. *Relationship between joint angles and joint torques*

The joints are driven by the force applied on the pulley. The joint torque is determined by the amount of pulling force T, the length of moment arm between the joint and the pulley, and the angle between the moment arm and the direction of pulling force. Higashimori et al. derived the torques for such a tendon-driven mechanism[4] with a single wire and actuator. In their study, the radius of the pulley is assumed to be non-zero, that is, the pulley was assumed to have a certain volume. For simple expression, in this paper, it was assumes that the radius of the pulley is infinitely small. Following this assumption, the relationship between the position of pulley and torques are expressed by modifying Higashimori's equation as

$$\begin{pmatrix} \tau_1 \\ \tau_2 \\ \tau_3 \end{pmatrix} = -T \begin{pmatrix} (\boldsymbol{p_1^a} - \boldsymbol{p_1}) \otimes \boldsymbol{e_1^b} - (\boldsymbol{p_2^a} - \boldsymbol{p_2}) \otimes \boldsymbol{e_2^b} \\ (\boldsymbol{p_2^a} - \boldsymbol{p_2}) \otimes \boldsymbol{e_2^b} - (\boldsymbol{p_3^a} - \boldsymbol{p_3}) \otimes \boldsymbol{e_3^b} \\ (\boldsymbol{p_3^a} - \boldsymbol{p_3}) \otimes \boldsymbol{e_3^b} \end{pmatrix}, \tag{1}$$

where p_i^a is the position vector of P_i^a, and p_j is that of P_j. e_i^b is a unit vector from P_i^a to P_{i-1}^a. $\otimes$ is the operator as

$$(x_1, y_1)^T \otimes (x_2, y_2)^T = x_1 y_2 - y_1 x_2$$

We assume that the weights of pulley and wire are zero, and the model is constructed on a sagittal plane.

2.3. *Simulation model*

To search an appropriate set of the position of the pulley, a simulation using the Open Dynamics Engine[5] was conducted. In the simulation, the size and mass of each link were determined, as in Table 1, supposing that the link is made of ABS, the density of which is lower than that of metal. The joint torque was calculated by following Equation (1). Figure 2 shows an illustration of the simulation. We supposed that a physical pneumatic actuator (SMC CDUJ6-30DM) is adopted as the linear actuator in the frame shown in Figure 1(a), and we set the tensional force T as 10 N by referring to the data sheet of the actuator.

Fig. 2. Snap shot of the simulation

Table 1. Link size (width × depth × height) [mm] and weight [g]

Link	Size [mm]	Weight [g]
Actuator	13.0 × 20.0 × 48.0	28
Trunk	10.0 × 20.0 × 125.0	17
Thigh	30.0 × 20.0 × 113.75	25
Shank	20.0 × 20.0 × 81.25	15
Foot	60.0 × 20.0 × 15.0	17

3. Simulation

3.1. *Simulation setup*

In the simulation, the positions of the pulley P_1^a and P_2^a were changed within a certain area, and we observed whether the model successfully achieves a jumping motion. The results of the test trials showed that the robot achieved the jumping motion successfully when the parameters were set within a certain range. Therefore, the parameters were searched for $0 \leq x_h \leq 30$, $-125 \leq y_h \leq -95$, $-15 \leq x_k \leq 15$, and $-238.75 \leq y_k \leq -208.75$ mm at 1.5 mm intervals. The height of a jump was determined as $min(max(z_p(t)), max(z_t(t)))$, where $z_p(t)$ is the height of the heel (pastern)

from the ground and $z_t(t)$ is that of the toe, $min(a, b)$ is smaller value of a and b, and $max(c(t))$ is highest value of c during the jump; that is, the height is defined as the smaller of the values of the highest position of the heel and toe. The position of P_0^a, the origin of pulling force, was fixed at (-11.5, -78.0). The position of the endpoint of the wire P_3^a was also fixed at (-15.0, -320.0). We observed whether the robot achieves successful jumping, i.e., it lifts off and lands without falling down, and whether the height of the jump is over 200 mm. Before its lift off, the angles of the robot's joints were set as $\theta_1 = 120°$, $\theta_2 = -100°$, and $\theta_3 = 140°$. In order to ready the robot for landing after lifting off, the joints were controlled with a small actuation as

$$\widehat{\tau_i} = -Kp_l(\theta_m - \theta_{dm}) - Kd_l\dot{\theta}_m,$$

where $\theta_m (m = 1, 2, 3)$ is the joint angle and θ_{dm} is the initial angle of the joints, that is, $\theta_{d1} = 120°$, $\theta_{d2} = -100°$, and $\theta_{d3} = 140°$. The gains Kp_l and Kd_l are sufficiently small not to hinder the torque generated by the pulling wire (Equation (1)), 0.01 Nm/rad and 0.001 Nm/(rad/s), respectively. Note that the torque $\widehat{\tau_i}$ and the torque τ_i explained in Equation(1) are added when the foot contacts on the ground, and only $\widehat{\tau_i}$ is added after the foot leaves the ground. We assumed that the mass of pulley is zero.

3.2. *Simulation results*

In the simulation, the parameters x_h, y_h, x_k, and y_k were varied, and the results showed that 658 sets of parameters allow the robot to jump successfully; that is, there exist 658 solutions in the 4 dimensional x_h, y_h, x_k, and y_k space. In the practical installation of the pulleys, a position error because of technical problems such as the radius of the hole to attach the pulley should be allowed. Therefore, among the 658 solutions in the four dimensions, we searched a group of solutions in which the distance between the neighbor solutions is very small, i.e., the position error is allowed. In order to search such an area, we adopted cluster analysis using Ward's method and Euclidean distance, and we did not perform normalization. Table 2 shows the means (M) and standard deviations (SD) of four larger clusters. The largest, and the second, third and fourth largest clusters contain 273, 165, 126, and 93 solutions, respectively. Those clusters are labeled as Cluster 1 to 4, respectively. The results indicate two points. One is that the areas that allow a position error are distributed. Considering that the position of the hip joint is $(0, -125)$ and that of the knee joint is $(0, -238.75)$, the distances of P_1^a from the hip joint in Cluster 1 and 3 are longer than

those in 2 and 4. The positions of P_k^a in Cluster 1 and 2 are set at the rear of the knee joint, and those in Cluster 3 and 4 are set at the front of the knee joint. The variation in the SD explains the allowance of each parameter. For example, in Cluster 3, the SD of x_k is larger than that of y_k. This means that the position error in this cluster is allowed along the horizontal direction and is not allowed to some degree along the vertical direction.

Table 2. Means and standard deviations of parameters

	x_h[mm] M(SD)	y_h[mm] M(SD)	x_k[mm] M(SD)	y_k[mm] M(SD)
Cluster 1	25.7(3.2)	-102.5(4.6)	-5.6(4.8)	-217.85(4.3)
Cluster 2	13.4(4.5)	-97.2(2.9)	-5.5(3.5)	-220.85(2.2)
Cluster 3	24.3(3.6)	-97.3(2.5)	8.6(4.3)	-223.75(2.3)
Cluster 4	14.0(5.9)	-100.4(4.6)	11.7(3.0)	-215.25(5.9)

4. Mathematical model

In the last section, we checked whether the proposed mechanism achieves successful jumping by utilizing the dynamics simulation. However, in order to investigate an appropriate set of pulley positions, it is important to derive a numerical model. In order to derive the numerical model, we have some assumption. On is that the model is constrained on the sagittal plane. The other is that the interaction between the robot and the ground is occurred instantly and the joint angles are not changed. We also have an assumption that the link moments are ignored. In order to derive a mathematical model of jumping, we applied an assumption that the joint angles are not changed during the lifting off motion and the reaction force is added at the toe because the interaction between the robot and the ground occurs instantaneously. We also applied the condition that the reaction force on the toe should be vertical and the projection of the center of mass (CoM) on the ground should correspond to the toe; otherwise, the robot tumbles while in the air. Based on this condition, the joint angles are strongly constrained, and we examined the position of the pulley that provides a vertical reaction force without a horizontal force being exerted on the toe following the assumption. Figure 3(a) shows the relationship between the joint torques and the force on the toe. The horizontal and vertical forces generated by the joint torque are expressed as F_x and F_y, respectively. Following the principle of virtual work, the relationship between the joint torque $(\tau_1, \tau_2, \tau_3)^T$ and $(F_x, F_y)^T$ is expressed as

$$\begin{pmatrix} \tau_1 \\ \tau_2 \\ \tau_3 \end{pmatrix} = \tau = {\mathbf{J}_\omega}^T \mathbf{R} \begin{pmatrix} F_x \\ F_y \end{pmatrix} . \; J_\omega = \begin{pmatrix} \frac{\partial x}{\partial \theta_1} & \frac{\partial x}{\partial \theta_2} & \frac{\partial x}{\partial \theta_3} \\ \frac{\partial y}{\partial \theta_1} & \frac{\partial y}{\partial \theta_2} & \frac{\partial y}{\partial \theta_3} \end{pmatrix}, \tag{2}$$

where (x, y) is the position of the toe. The elements of matrix J_ω are expressed from

$$x = l_2 \sin\theta_1 + l_3 \sin(\theta_1 + \theta_2) + l_4 \sin(\theta_1 + \theta_2 + \theta_3),$$
$$y = -l_1 - l_2 \cos\theta_1 - l_3 \cos(\theta_1 + \theta_2) - l_4 \cos(\theta_1 + \theta_2 + \theta_3)$$

$\mathbf{R}$ is the rotation matrix from the force based on Σ_0 to $(F_x, F_y)^T$,

$$\mathbf{R} = \begin{pmatrix} \sin\Theta & \cos\Theta \\ -\cos\Theta & \sin\Theta \end{pmatrix}, \quad \Theta = \theta_1 + \theta_2 + \theta_3.$$

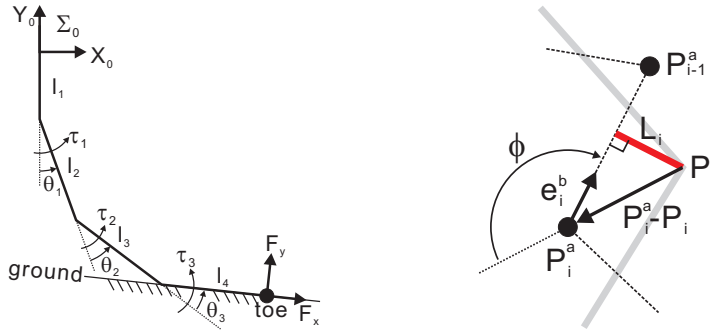

(a) Force applied on the toe $(F_x, F_y)^T$

(b) Distance from joint to the line between P_i^a and P_{i-1}^a

Fig. 3. Posture of the model and distance between the joint and the wire

Considering that the vector $\mathbf{e}_i^b$ in Equation (1) is the unit vector, the term of $(\mathbf{p}_i^a - \mathbf{p}_i) \otimes \mathbf{e}_i^b (i = 1, 2, 3)$ is deformed as

$$(\mathbf{p}_i^a - \mathbf{p}_i) \otimes \mathbf{e}_i^b = |\mathbf{p}_i^a - \mathbf{p}_i| \sin\phi \stackrel{\text{def}}{=} L_i, \tag{3}$$

where ϕ is the angle between $\mathbf{p}_i^a - \mathbf{p}_i$ and $\mathbf{e}_i$ (see Figure 3(b)). Therefore, the term L_u is expressed by the length between the line of P_{i-1}^a and P_i^a and the joint P_i. By substituting $F_x = 0$, in which the horizontal force does not occur, the length of L_i is expressed as

$$\begin{pmatrix} L_1 - L_2 \\ L_2 - L_3 \\ L_3 \end{pmatrix} = K \begin{pmatrix} l_2 \cos(\theta_2 + \theta_3) + l_3 \cos\theta_3 + l_4 \\ l_3 \cos\theta_3 + l_4 \\ l_4 \end{pmatrix}, \tag{4}$$

where $K = -F_y/T > 0$ is the ratio of the force of pulling wire T and the reaction force from the ground $-F_y$. From the third row, the length L_3 is obtained when K is determined. From the second row, L_2 is automatically

obtained when the joint angles that satisfy the condition of the CoM are determined. From the first row, L_3 is also obtained. Because the positions of end points P_0^a and P_3^a are fixed, the positions of P_1^a and P_2^a are strongly constrained by the condition of L_1, L_2, and L_3. For example, position P_2^a should be set so that the distance between the line of P_3^a and P_2^a and the joint P_3 is L_3. Therefore, we conclude that the candidate positions of the pulley that generates vertical force are limited when the value of K is set.

5. Conclusion

This paper addressed a legged jumping robot, the joints of which are driven by a single wire and actuator. The wire passes through pulleys attached on each link and the joints are driven by pulling the wire. Although the weight of this mechanism is appropriate and the mechanism is simple and compact, the positions of pulley influence the dynamic behavior. This paper suggested a design principle for a tendon-driven joint mechanism considering of a single wire and actuator set for vertical jumping. A simulation utilizing a physical engine showed that there are some areas that allow an error in the position of the pulleys, which will facilitate the practical development of the robot. We also found that the area is not isotropic and an error is allowed along a certain direction and is not allowed in some extent along the other direction. We also derived a procedure for determining the appropriate pulley positions. In order to verify the validity of the simulation results and mathematical models, we intend to develop a physical robot in the future.

References

1. F. Günther, F. Giardina, and F. Iida. Self-stable one-legged hopping using a curved foot. In *Proceedings of 2014 IEEE International Conference on Robotics and Automation*, pages 5133–5138, 2014.
2. S. Kitano, S. Hirose, G. Endo, and E. F. Fukushima. Development of lightweight sprawling-type quadruped robot TITAN-XIII and its dynamic walking. In *Proceedings of 2013 IEEE/RSJ International Conference on Intelligent Robots and Systems*, pages 6025–6030, November 2013.
3. S. Cotton, I. M. C. Olaru, M. Bellman, T. van. der. Ven, J. Godowski, and J. Pratt. FastRunner: A fast, efficient and robust bipedal robot. concept and planar simulation. In *Proceedings of 2012 IEEE International Conference on Robotics and Automation*, pages 2358–2364, 2012.
4. M. Higashimori, M. Kaneko, A. Namiki, and M. Ishikawa. Design of the 100G capturing robot based on dynamic preshaping. *International Journal of Robotics Research*, 24(9):743–753, 2005.
5. *ODE Home Page*. http://www.ode.org/.